# [2]Rotaxanes featuring minimal helical axles

Jorge Meijide Suárez,[1,*] Vicente Martí-Centelles,[1] Arnaud Tron,[1] Thierry Buffeteau,[1] Stéphane Massip,[2] Céline Olivier,[1] Isabelle Pianet,[3] Cybille Rossy,[1] Jean-Marc Vincent,[1] Nathan D. McClenaghan[1,*]

[1]Univ. Bordeaux, CNRS, Bordeaux INP, ISM, UMR 5255, F-33400 Talence, France
[2]Univ. Bordeaux, CNRS, INSERM, IECB, US1, UAR 3033, F-33600 Pessac, France
[3]Iramat-CRP2A, Université Bordeaux Montaigne

*Corresponding authors:
nathan.mcclenaghan@u-bordeaux.fr (NMcC); jorge.meijide-suarez@u-bordeaux.fr (JMS)

Keywords: Rotaxane, dynamic NMR, V-CD, chirality, supramolecular chemistry.

ABSTRACT: α,ω-Stoppered perfluorous domains act as rigid and chiral linear helical elements in rotaxane constructs. Dynamic NMR shows modified ring dynamics over 4–orders of magnitude compared to hydrocarbon analogues, while vibrational-CD shows stopper-induced preferential axle chirality.

Rotaxanes have emerged as versatile architectures in the development of interlocked structures and artificial molecular machines. Indeed, mechanical stoppering of the macrocycle on the thread adds new features to the entire structure that offers function from the molecular to the macromolecular level.[1,2,3] External stimuli may be used to control the affinity of the macrocycle for different chemical functions on the thread to control its position and be applied in on-off switches,[4] electron transport,[5] catalysis[6] or the synthesis of highly enantioenriched mechanically planar chiral rotaxanes.[7]

Controlling the movement and dynamics of a macrocycle along a thread are the key feature on the development of interlocked-based molecular machines. During the last years, examples of directional threading,[8,9] energy ratchets[10,11] and speed bumps[12] are different approaches to control the movement of a macrocycle within an interlocked structure. Previous studies show a dependence on the number of stations and macrocycles,[13] in the case of [2]rotaxanes with more than one station, the macrocycle is preferentially positioned at the highest affinity station,[14] if the affinity between both stations is the same, the macrocycle will be in constant movement between the stations.[15] Globally, observed properties are intimately linked to the constituent molecular components, including stoppers, macrocycles and axles.

By far the most widely employed axles are aliphatic, typically hydrocarbon or ethylene glycol oligomers, rendering the resultant structures highly flexible.[12,16,17,18] A few reports, consider more structurally-elaborate rigid axles, offering a more well-defined ring trajectory along the axle.[19,20,21] The nature of the rigid linker is typically aromatic[20,22] or acetylenic,[21] which can necessitate multi-step synthesis and/or introduce π-conjugated systems which may be redox active and introduce low-lying excited states which may, for instance, result in unwanted rotaxane luminescence quenching.[23]

Despite the continued interest in introducing fluorinated groups and sub-units to change the properties of organic compounds, including solubility and pharmacokinetics, integrating fluorinated segments in rotaxanes has been scarcely considered. Leigh introduced a $-(CF_2)_2-$ group as a rotaxane ring station to modulate rotaxane hydrophobicity,[24] Lüning reported grafting a pendant fluorous ponytail onto a ring component to change solubility and effect proton transport,[25] while Coutrot reported a short terminal fluorous ponytail which affected ring dissociation froma pseuodorotaxane axle.[26]

We reasoned that intoducing a central perfluorinated domain in a rotaxane would offer an inert and atom-economical means to introduce a rigid rotaxane axle. Indeed, due to stereoelectronic repulsions between fluorine atoms, perfluorous chains are considered more rigid than hydrocarbon ones,

possessing dihedral angles of 162°.[27] These well defined angles induce helical structures, whose handedness (P or M) is sensitive to the local chiral environment.[28]
Herein we report [2]rotaxanes bearing short (-$C_6F_{12}$-) fluorinated domains which provide a well-defined helical axle and study kinetics of ring shuttling with rings of different size, as well as induction of enantioenrichment via enantiopure stopper groups and transmission of chirality, compared to analogues with hydrocarbon chains (Figure 1).

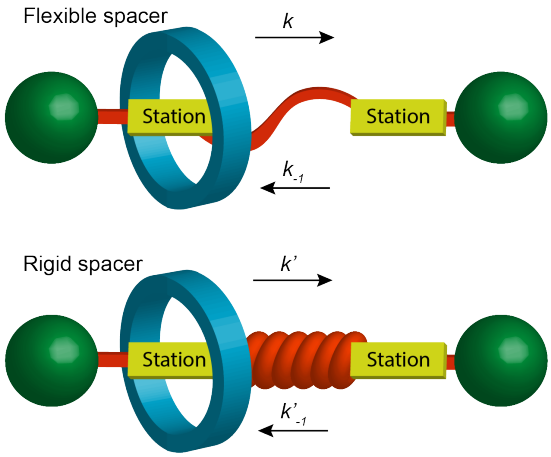


*Figure 1: Cartoon representation of rotaxanes studied in this work.*

In order to identify the effects of each component of the structure on the properties, five different rotaxanes were synthesized. They all possess two identical stations to avoid affinity interferences. Rotaxanes **XX-1** and **XX-2** contain both a hydrocarbon -$C_6H_{12}$- spacer and one different macrocycle each, both with the same number of atoms (27). The same macrocycles were integrated in rotaxanes **XX-3** and **XX-4** but the hydrocarbon chain is replaced by a -$C_6F_{12}$- spacer. Equally, in order to study the chirality, half threads and thread **XX-5** and **XX-6** were synthesized and analyzed by vibrational circular dichroism (V-CD) to understand the nature of the signals obtained for rotaxane **XX-7**.

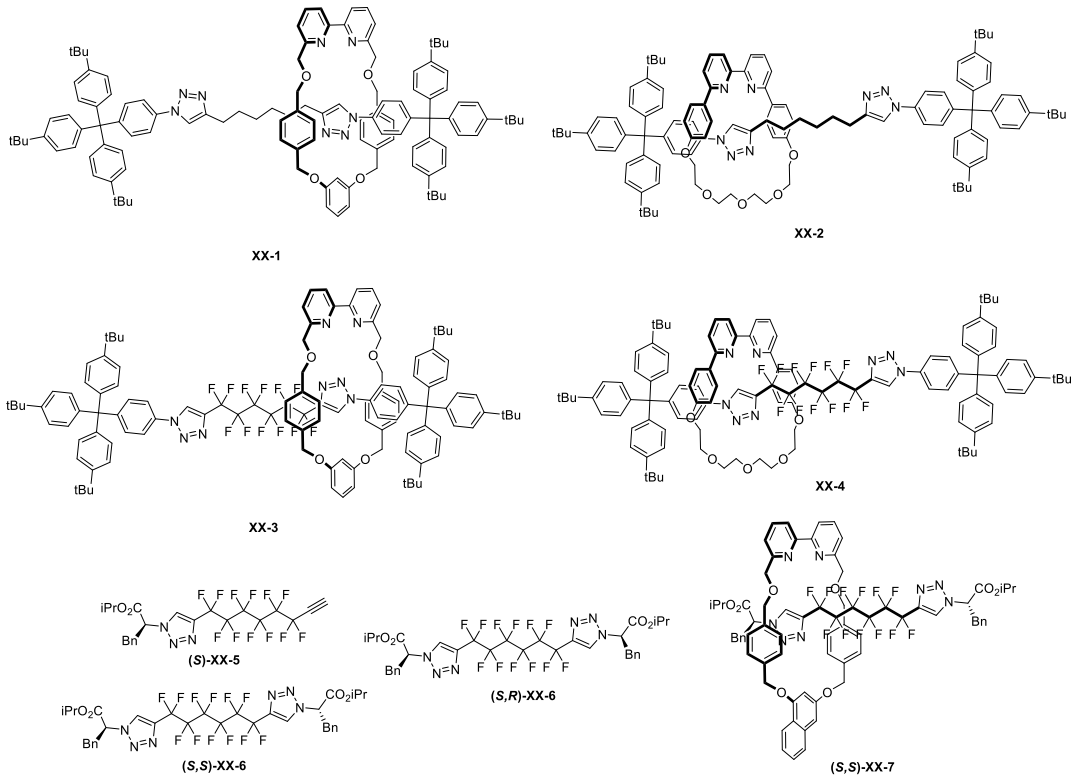


*Figure 2: Rotaxanes and axles studied in this work.*

The rotaxanes were synthesized by $Cu^{I}$ catalyzed active template with the corresponding half threads[29] (see Supplementary Information, SI). **XX-1** and **XX-2** contain the same $C_6H_{12}$ hydrocarbon thread but different macrocycles. **XX-3** and **XX-4** contain the same respective macrocycles but the spacer was replaced by -$C_6F_{12}$-. Similar qualitative results were observed for **XX-1** and **XX-2** in $^1$H-NMR, none of them show deshielded triazole protons, characteristic of low residence times of the macrocycle on the station. Additionally, an overall symmetry can easily be observed since no equivalent benzylic $CH_2$ are observed for the macrocycle, showing a fast exchange on the NMR timescale at room temperature (Figure 3a represented for **XX-1**). Coalescence was not reached at low temperature NMR (Supplementary Information Figure S46). On the other hand, analogues **XX-3** and **XX-4** integrating perfluorinated domains show two different triazole proton resonances, one of them extremely deshielded characteristic of a H-bond interaction with the triazole (Figure 3b represented for **XX-3**).[7] Additionally, diastereotopic benzylic $CH_2$ of the macrocycle, characteristic of a non-equivalency due to the threading coupled to a slow shuttling in the NMR timescale.

Exchange was confirmed by NOESY where cross correlations are observed between both triazoles (Figure 3c). Additionally, NOESY run at different $\tau_{mix}$ allowed the EXSY analysis of the data and kinetic constants were calculated (Figure 3d). Two very different rates were observed for both rotaxanes, $k_{(XX\text{-}3)}$ = 14.8 $ms^{-1}$ and $k_{(XX\text{-}4)} = 3.71 \times 10^5$ $ms^{-1}$ showing, not only a slowing down of shuttling across the the rigid and relatively bulky -$C_6F_{12}$- spacer but also a dramatic dependence on the shape of the macrocycle (data summarized in Table 1).

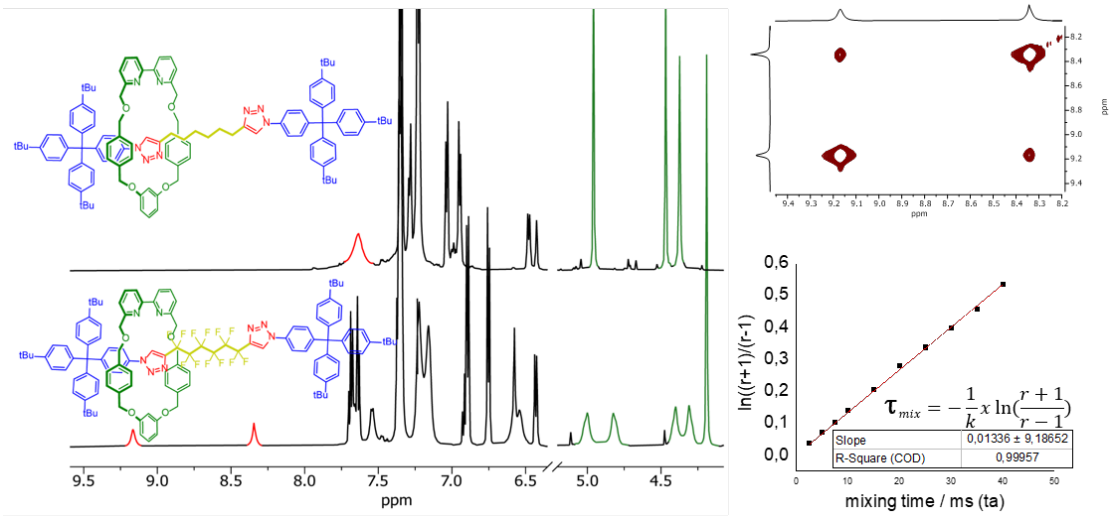


*Figure 3: a) $^1$H-NMR of **XX-1**. $CD_2Cl_2$, 298 K, b) $^1$H-NMR of **XX-3**. $CD_2Cl_2$, 298, c) extract of NOESY spectra of XX-3, 600 MHz, $CD_2Cl_2$, 298 K d) Determination of ring shuttling rate from EXSY data.*

Table 1: Results of ring shuttling kinetics from NMR data.

| Rotaxane | Rate |
|---|---|
| **XX-1** | Above coalescence at low temperature |
| **XX-2** | Above coalescence at low temperature |
| **XX-3** | $k$ = 14.8 $ms^{-1}$ |
| **XX-4** | $k$ = 3.71 x $10^5$ $ms^{-1}$ |

In order to introduce a preferential chirality in the fluorinated rotaxane structures, which exist as racemates, a phenylalanine-azide derivative was introduced in the synthesis of both the half threads (***S***)-**XX-5** and (***R***)-**XX-5**, as well as the entire thread (***S,S***)-**XX-6** and (***R,R***)-**XX-6**. V-CD analysis shows the characteristic signals at 1200 $cm^{-1}$ corresponding to the perfluorinated, chain confirming the transmission of the chirality from the chiral phenyl-alanine to the helical -$C_6F_{12}$- chain across the triazole (Figure 4). The increase of intensity on the V-CD signals from **XX-5** to **XX-6** suggest that the helicity is not conserved all along the chain, and is eventually lost halfway through. (For a more complete attribution of signals of the IR spectrum, see Figure S49 and S50 of the SI).

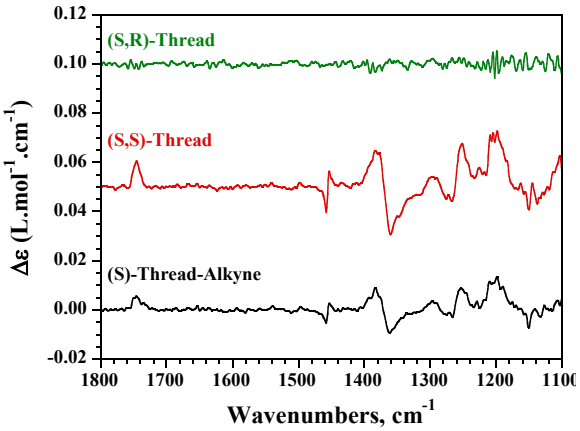


*Figure 4: V-CD spectra of (S)-**XX-5** and (S)-**XX-6** in $CD_2Cl_2$.*

Rotaxanes (***S,S***)-**XX-7** and (***R,R***)-**XX-7** were synthesized by the same active template methodology, (see SI). However, it is noteworthy that non-symmetrical rotaxanes could be obtained by sequential

cycloaddition reactions, increasing the scope of rotaxane architectures that could be developed. Some perturbations are observed in the V-CD spectrum. A very small negative contribution at 1600 $cm^{-1}$ corresponding to the naphthalene on the macrocycle. A very strong negative contribution that cancels the positive one at 1450 $cm^{-1}$, corresponding to the bipyridine on the macrocycle.[30] Negative contributions are observed around the 1350 $cm^{-1}$. Disruptions along the window of 1350 $cm^{-1}$ were observed, which corresponds to new signals of the IR spectrum corresponding to the interlocked structure (double bonds of the bipyridine). Additionally, a strong positive contribution at 1240 $cm^{-1}$ is also observed, this last band was previously attributed to the ethers of the macrocycle.[30]

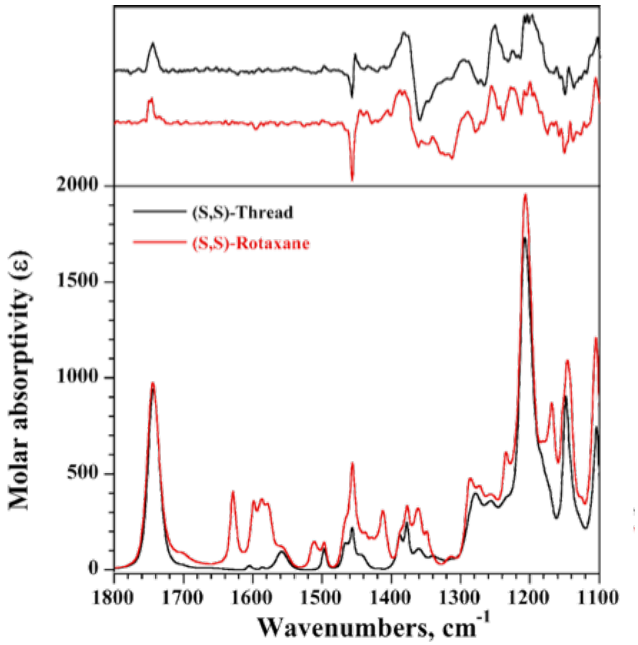


*Figure 5: V-CD spectra of (S,S)-XX-6 (black) and (S,S)-XX-7. $CD_2Cl_2$*

As an additional proof of chirality transfer from the helical thread to the macrocycle, Electronic Circular dichroism was recorded for rotaxanes **(*S,S*)-XX-7** and **(*R,R*)-XX-7**. The spectra show a single band below 300 nm corresponding to the bipyridine of the macrocycle. This result confirms the information obtained from the V-CD spectra, that the transmission of chirality is occurring from the helical thread to the macrocycle.

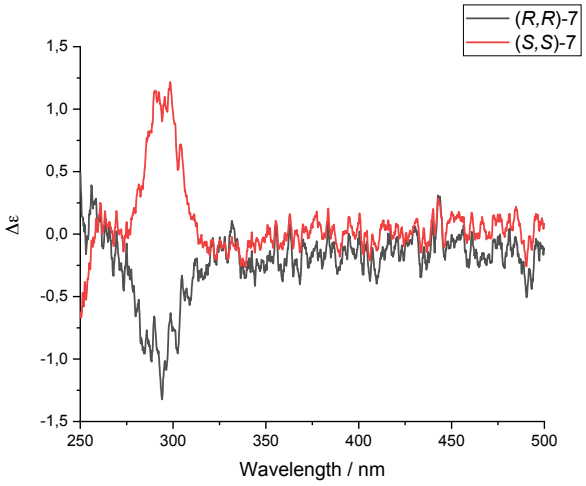


*Figure 6: E-CD spectra of (R,R)-**XX-7** and (S,S)-**XX-7** in $CHCl_3$.*

In conclusion, this work shows that perfluorinated domains can be readily integrated as inert, rigid axles in the synthesis of both symmetrical and non-symmetrical rotaxanes. Profound effects on the

shuttling rates of macrocycles in such rotaxanes with more than one station compared to hydrocarbon chain-containing analogues are noted, while macrocycles with different shapes can tune the speed of ring movement over 4-orders of magnitude. Additionally, the use of chiral stoppers showed the transmission of chiral induction through the triazole to the -$C_6F_{12}$- chain, which also allowed the study of the transmission of the chirality from the helical thread to the prochiral macrocycle in a dynamic rotaxane for the first time. Ongoing work focuses on extending chiral transmission in perfluorinated domains and developing hybrid hydrocarbon-perfluorinated architectures.

(1) Mena-Hernando, S.; Pérez, E. M. Mechanically Interlocked Materials. Rotaxanes and Catenanes beyond the Small Molecule. *Chem. Soc. Rev.* **2019**, *48* (19), 5016–5032. https://doi.org/10.1039/C8CS00888D.
(2) De Bo, G. Mechanochemistry of the Mechanical Bond. *Chem. Sci.* **2018**, *9* (1), 15–21. https://doi.org/10.1039/C7SC04200K.
(3) Takata, T. Switchable Polymer Materials Controlled by Rotaxane Macromolecular Switches. *ACS Cent. Sci.* **2020**, *6* (2), 129–143. https://doi.org/10.1021/acscentsci.0c00002.
(4) Blanco, V.; Leigh, D. A.; Marcos, V. Artificial Switchable Catalysts. *Chem. Soc. Rev.* **2015**, *44* (15), 5341–5370. https://doi.org/10.1039/C5CS00096C.
(5) Kwan, P. H.; Swager, T. M. Intramolecular Photoinduced Charge Transfer in Rotaxanes. *J. Am. Chem. Soc.* **2005**, *127* (16), 5902–5909. https://doi.org/10.1021/ja042535o.
(6) Heard, A. W.; Suárez, J. M.; Goldup, S. M. Controlling Catalyst Activity, Chemoselectivity and Stereoselectivity with the Mechanical Bond. *Nat. Rev. Chem.* **2022**. https://doi.org/10.1038/s41570-021-00348-4.
(7) de Juan, A.; Lozano, D.; Heard, A. W.; Jinks, M. A.; Suarez, J. M.; Tizzard, G. J.; Goldup, S. M. A Chiral Interlocking Auxiliary Strategy for the Synthesis of Mechanically Planar Chiral Rotaxanes. *Nat. Chem.* **2021**. https://doi.org/10.1038/s41557-021-00825-9.
(8) Oshikiri, T.; Yamaguchi, H.; Takashima, Y.; Harada, A. Face Selective Translation of a Cyclodextrin Ring along an Axle. *Chem. Commun.* **2009**, No. 37, 5515. https://doi.org/10.1039/b906425g.
(9) Oshikiri, T.; Takashima, Y.; Yamaguchi, H.; Harada, A. Kinetic Control of Threading of Cyclodextrins onto Axle Molecules. *J. Am. Chem. Soc.* **2005**, *127* (35), 12186–12187. https://doi.org/10.1021/ja053532u.
(10) Alvarez-Pérez, M.; Goldup, S. M.; Leigh, D. A.; Slawin, A. M. Z. A Chemically-Driven Molecular Information Ratchet. *J. Am. Chem. Soc.* **2008**, *130* (6), 1836–1838. https://doi.org/10.1021/ja7102394.
(11) Serreli, V.; Lee, C.-F.; Kay, E. R.; Leigh, D. A. A Molecular Information Ratchet. *Nature* **2007**, *445* (7127), 523–527. https://doi.org/10.1038/nature05452.
(12) Douarre, M.; Martí-Centelles, V.; Rossy, C.; Pianet, I.; McClenaghan, N. D. Regulation of Macrocycle Shuttling Rates in [2]Rotaxanes by Amino-Acid Speed Bumps in Organic–Aqueous Solvent Mixtures. *Eur. J. Org. Chem.* **2020**, *2020* (36), 5820–5827. https://doi.org/10.1002/ejoc.202000997.
(13) Zhu, K.; Baggi, G.; Loeb, S. J. Ring-through-Ring Molecular Shuttling in a Saturated [3]Rotaxane. *Nat. Chem.* **2018**, *10* (6), 625–630. https://doi.org/10.1038/s41557-018-0040-9.
(14) Curcio, M.; Nicoli, F.; Paltrinieri, E.; Fois, E.; Tabacchi, G.; Cavallo, L.; Silvi, S.; Baroncini, M.; Credi, A. Chemically Induced Mismatch of Rings and Stations in [3]Rotaxanes. *J. Am. Chem. Soc.* **2021**, *143* (21), 8046–8055. https://doi.org/10.1021/jacs.1c02230.
(15) Corra, S.; de Vet, C.; Groppi, J.; La Rosa, M.; Silvi, S.; Baroncini, M.; Credi, A. Chemical On/Off Switching of Mechanically Planar Chirality and Chiral Anion Recognition in a [2]Rotaxane Molecular Shuttle. *J. Am. Chem. Soc.* **2019**, *141* (23), 9129–9133. https://doi.org/10.1021/jacs.9b00941.
(16) Kang, S.; Vignon, S. A.; Tseng, H.-R.; Stoddart, J. F. Molecular Shuttles Based on Tetrathiafulvalene Units and 1,5-Dioxynaphthalene Ring Systems. *Chem. – Eur. J.* **2004**, *10* (10), 2555–2564. https://doi.org/10.1002/chem.200305725.
(17) Günbaş, D. D.; Brouwer, A. M. Degenerate Molecular Shuttles with Flexible and Rigid Spacers. *J. Org. Chem.* **2012**, *77* (13), 5724–5735. https://doi.org/10.1021/jo300907r.
(18) *Molecular Shuttles by the Protecting Group Approach | The Journal of Organic Chemistry*. https://pubs.acs.org/doi/pdf/10.1021/jo991397w (accessed 2023-01-03).
(19) Fadler, R. E.; Flood, A. H. Rigidity and Flexibility in Rotaxanes and Their Relatives; On Being Stubborn and Easy-Going. *Front. Chem.* **2022**, *10*, 856173. https://doi.org/10.3389/fchem.2022.856173.
(20) Sleiman, H.; Baxter, P.; Lehn, J.-M.; Rissanen, K. Self-Assembly of Rigid-Rack Multimetallic

Complexes of Rotaxane-Type. *J. Chem. Soc. Chem. Commun.* **1995**, No. 7, 715. https://doi.org/10.1039/c39950000715.
(21) Nygaard, S.; Leung, K. C.-F.; Aprahamian, I.; Ikeda, T.; Saha, S.; Laursen, B. W.; Kim, S.-Y.; Hansen, S. W.; Stein, P. C.; Flood, A. H.; Stoddart, J. F.; Jeppesen, J. O. Functionally Rigid Bistable [2]Rotaxanes. *J. Am. Chem. Soc.* **2007**, *129* (4), 960–970. https://doi.org/10.1021/ja0663529.
(22) Gholami, G.; Zhu, K.; Baggi, G.; Schott, E.; Zarate, X.; Loeb, S. J. Influence of Axle Length on the Rate and Mechanism of Shuttling in Rigid H-Shaped [2]Rotaxanes. *Chem Sci* **2017**, *8* (11), 7718–7723. https://doi.org/10.1039/C7SC03736H.
(23) Movsisyan, L. D.; Kondratuk, D. V.; Franz, M.; Thompson, A. L.; Tykwinski, R. R.; Anderson, H. L. Synthesis of Polyyne Rotaxanes. *Org. Lett.* **2012**, *14* (13), 3424–3426. https://doi.org/10.1021/ol301392t.
(24) Berná, J.; Leigh, D. A.; Lubomska, M.; Mendoza, S. M.; Pérez, E. M.; Rudolf, P.; Teobaldi, G.; Zerbetto, F. Macroscopic Transport by Synthetic Molecular Machines. *Nat. Mater.* **2005**, *4* (9), 704–710. https://doi.org/10.1038/nmat1455.
(25) Beyer, O.; Hesseler, B.; Lüning, U. A Convenient Access to a [2]Rotaxane Proton Shuttle by Using a Fluorous Ponytail. *Synthesis* **2015**, *47* (16), 2485–2495. https://doi.org/10.1055/s-0034-1380814.
(26) Gauthier, M.; Coutrot, F. Discrepancy Regarding the Dethreading of a Dibenzo-24-Crown-8 Macrocycle through a Perfluorobutyl End in [2]Pseudorotaxanes. *Eur. J. Org. Chem.* **2022**, *2022* (21), e202101201. https://doi.org/10.1002/ejoc.202101201.
(27) Jang, S. S.; Blanco, M.; Goddard, W. A.; Caldwell, G.; Ross, R. B. The Source of Helicity in Perfluorinated *N* -Alkanes. *Macromolecules* **2003**, *36* (14), 5331–5341. https://doi.org/10.1021/ma025645t.
(28) Monde, K.; Miura, N.; Hashimoto, M.; Taniguchi, T.; Inabe, T. Conformational Analysis of Chiral Helical Perfluoroalkyl Chains by VCD. *J. Am. Chem. Soc.* **2006**, *128* (18), 6000–6001. https://doi.org/10.1021/ja0602041.
(29) Denis, M.; Goldup, S. M. The Active Template Approach to Interlocked Molecules. *Nat. Rev. Chem.* **2017**, *1* (8), 1–17. https://doi.org/10.1038/s41570-017-0061.
(30) Koenis, M. A. J.; Chibueze, C. S.; Jinks, M. A.; Nicu, V. P.; Visscher, L.; Goldup, S. M.; Buma, W. J. Vibrational Circular Dichroism Spectroscopy for Probing the Expression of Chirality in Mechanically Planar Chiral Rotaxanes. *Chem. Sci.* **2020**, *11* (32), 8469–8475. https://doi.org/10.1039/D0SC02485F.